THE JOURNAL OF PHYSICAL CHEMISTRY B

 VOLUME 104, NUMBER 31, AUGUST 10, 2000

LETTERS

Convergence of Molecular and Macroscopic Continuum Descriptions of Ion Hydration

Henry S. Ashbaugh[†]

Department of Chemical Engineering, Princeton University, The Engineering Quadrangle, Olden St., Princeton, New Jersey 08544-5263

Received: April 20, 2000; In Final Form: June 13, 2000

Using computer simulations we study the boundary between explicit molecular and macroscopic continuum dielectric descriptions of ion hydration. The continuum model reasonably describes electrostatic potential fluctuation contributions to the hydration free energy, but fails to capture first-order potential contributions in the uncharged state. Once this contribution is accounted for, cationic and anionic free energies become indistinguishable with increasing size, in agreement with continuum model predictions. The ion radius at which the hydration free energies converge scales as the square root of the absolute charge ($\upsilon = 0.54 \pm 0.04$) and compares to the length scale ion−water dipole interactions equal the thermal energy.

On a macroscopic and molecular level, theoretical descriptions of the hydration of charged surfaces and ions are fundamentally different. On a macroscopic scale where the interactions of individual molecules are inconsequential, water can be treated as a linearly polarizable dielectric continuum. On a microscopic scale where strong specific interactions such as hydrogen bonding play an intimate role in hydration, explicit molecular interactions must be taken into account. The boundary between these extreme descriptions of water is poorly understood. Nevertheless, the conceptional and computational simplicity of the continuum dielectric model has motivated its application to molecular level phenomena ranging from the correlation of solute transfer free energies to biomolecular assembly and stability.[1]

Applied to the hydration of a single spherical monatomic ion, the continuum model yields the Born equation for the ion charging free energy[2]

$$\mu^*(0\rightarrow q) = -q^2(1 - 1/\epsilon)/2R_B \qquad (1)$$

The ion charge, q, and solvent dielectric constant, ϵ, are determined by the experimental conditions, leaving the Born radius, R_B, as a single phenomenological parameter encapsulating all uncertainties over treating water as a structureless continuum. The success of the Born equation at correlating ion solubilities has stimulated theoretical efforts to understand its molecular implications in the hope that similar simplifications can be exploited for more complex species. From statistical thermodynamic considerations, the first and second derivatives of the free energy with respect to charge are related to the average and fluctuation in the solvent induced electrostatic potential[3−5]

$$\begin{aligned} d\mu^*/dq &= \langle\Phi\rangle_q \\ d^2\mu^*/dq^2 &= -\beta(\langle\Phi^2\rangle_q - \langle\Phi\rangle_q{}^2) \end{aligned} \qquad (2)$$

where $\beta^{-1} = kT$ is the product of Boltzmann's constant and the absolute temperature, while the brackets $\langle ... \rangle_q$ denote ensemble averages at charge q. Third- and higher-order derivatives are equal to zero for the continuum model. For monatomic[3] and molecular[6] ions in aqueous solution, however, $\langle\Phi\rangle_q$ is piecewise linear with a slope that depends on the sign of q.[7,8] More significant deviations from linear charging in water have been observed for polar solutes, notably water as a solute

[†] E-mail: hank@princeton.edu.

10.1021/jp0015067 CCC: $19.00
Published on Web 07/19/2000

itself.[5,7−10] The above statistical thermodynamic expressions, however, provide no insight into the relationship between the ion size and the free energy. While the Born equation presumes they are inversely proportional, eq 1 serves merely as a definition of R_B. The phenomenological character of R_B has been realized since its inception, as exemplified by Latimer et al. who ascribed consistently greater radii to cations over comparably sized anions in water.[11] That is, anions are more favorably hydrated than cations, in contrast to the prediction that the free energy depends only on the magnitude of the ion charge. Recent effort has focused on correlating R_B with either electronic structure or solvent densities in the solvation shell, though an unambiguous interpretation is unlikely.[12−15] In this Letter, we report explicit molecular simulation calculations of hard-sphere ion hydration free energies to explore the relationship between the physical ion size, charge, and the continuum model. Our results demonstrate, for the first time, that while anion and cation hydration is distinct on a molecular scale, water does not discriminate between oppositely charged species for larger ions, bridging the gap between these extreme representations of water.

Monte Carlo (MC) simulations of a single hard-sphere ion in water were performed to assess the effect of ion radius on the charging free energy. Spherical ions up to 9.85 Å in radius R were examined, where R denotes the distance of closest approach between the ion and water oxygen centers. While such large ions may be physically untenable, this size range allows us to critically assess the Born equation from molecular toward macroscopic scales where the continuum approximation is accurate. Water was modeled using the simple point charge potential (SPC).[16] Simulations were performed in the canonical ensemble at 25 °C and the simulation volume was adjusted so that the water density in the corners of the periodic cell was 0.997 g/cm^3 ± 0.5%. For ions smaller than 6 Å, 216 water molecules were included in the calculation, while 471 and 1435 water molecules were considered with the 7.45 and 9.85 Å radius ions, respectively. Nine charge states from $-2e$ to $+2e$ in $+0.5e$ increments were examined. From the average and fluctuation in the electrostatic potential, the charging free energy difference between consecutive charge states, $\delta q = q_{i+1} - q_i$, is

$$\mu^*(q \rightarrow q+\delta q) = (\delta q/2)(\langle\Phi\rangle_q + \langle\Phi\rangle_{q+\delta q}) - (\beta\delta q^2/12)[(\langle\Phi^2\rangle_q - \langle\Phi\rangle_q{}^2) - (\langle\Phi^2\rangle_{q+\delta q} - \langle\Phi\rangle_{q+\delta q}{}^2)] \quad (3)$$

assuming the potential is a cubic function of charge.[17] Long-range electrostatic interactions were evaluated using Ewald summation with conducting boundary conditions ($\epsilon_{boundary} = \infty$).[18] The electrostatic potential was measured relative to bulk water, owing to normalization of the Ewald potential.[3,19] In addition to self-interaction terms,[3] additional corrections accounting for the periodicity of the simulation cell and the finite aqueous dielectric constant ($\epsilon_{SPC} = 65$) were included in the calculation of the free energy.[20,21] After equilibration, 10^5 MC moves were attempted for each water molecule to evaluate thermodynamic averages.

As observed experimentally, anion hydration is favored over cation hydration, indicated by the consistently lower values of R_B ascribed to anions (Figure 1). The Born radii of monovalent ions are increasing functions of size, although the relationship is not linear as might be expected. Indeed, the cationic R_B diverge with increasing size, while the results suggest the anionic R_B plateau at a finite asymptote. The reasons for this can be traced to the electrostatic potential at the center of an uncharged ion, $\langle\Phi\rangle_0$. While the continuum model predicts $\langle\Phi\rangle_0 = 0$, this

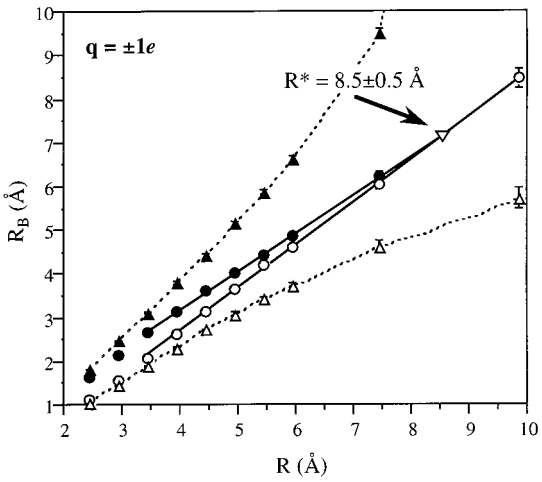

Figure 1. Born radii of monovalent ions determined from charging free energies. The closed and open triangles denote R_B for cations and anions, respectively, evaluated directly from simulation. The closed and open circles denote R_B for cations and anions, respectively, determined after correcting the free energy by subtracting $q\langle\Phi\rangle_0$ from the simulation free energy. The open upside down triangle denotes $R = R^*$ where the corrected cationic and anionic R_B converge. The lines are only guides for the eyes. The error bars denote 1 standard deviation.

is not required. Indeed it is shown below that $\langle\Phi\rangle_0$ is finite, positive, and only a weak function of increasing ion size. Assuming potential fluctuations are independent of q,[22] the charging free energy is $\mu^*(0 \rightarrow q) \approx q\langle\Phi\rangle_0 - \beta q^2(\langle\Phi^2\rangle - \langle\Phi\rangle^2)/2$. When $\langle\Phi\rangle_0$ is positive, the charging free energy for cations is zero when $(\langle\Phi^2\rangle - \langle\Phi\rangle^2) = 2\langle\Phi\rangle_0/\beta q$, at which point R_B diverges. Conversely for anions, the Born radius plateaus at $R_B = q(1 - \epsilon)/2\epsilon\langle\Phi\rangle_0$ as $R \rightarrow \infty$ assuming potential fluctuations are negligible in this limit.[22] These unphysical results can be avoided if $q\langle\Phi\rangle_0$ is subtracted from the free energy. First, however, we consider $\langle\Phi\rangle_0$ in detail.

The potential at zero charge rapidly increases with size from zero, corresponding to bulk water, to a maximum at sizes comparable to the OH bond length, $R_{OH} = 1$ Å (Figure 2). Assuming water is randomly oriented with respect to the solute, the electrostatic potential interaction of the solute with a water molecule averaged about the oxygen is

$$\varphi(r) = 2q_H\left(\frac{1}{R_{OH}} - \frac{1}{R}\right) \qquad \text{for } r < R_{OH} \text{ and 0 otherwise} \quad (4)$$

where q_H ($=+0.41e$ for SPC water) is the hydrogen charge, and r is the separation between the solute and water oxygen centers. Assuming solute−water oxygen correlations are described by a step function, i.e., $g_{sw} = 0$ for $r < R$ and 1 for $r > R$, $\langle\Phi\rangle_0$ measured relative to bulk water is

$$\langle\Phi\rangle_0 = 8\pi\rho_w q_H\left(\frac{R^2}{2} - \frac{R^3}{R_{OH}}\right) \qquad \text{for } R < R_{OH} \quad (5)$$

where ρ_w is the density of water. This expression accurately describes the initial increase in the potential, although it marginally overshoots the observed maximum owing to the breakdown of the random orientation assumption (Figure 2). Opening a cavity in water generates a region of average positive potential that repels water hydrogens, in turn lowering the solute's potential.

For larger solutes ($R > 1$ Å), water forms a hydrogen-bonded cage about the solute where the bond vectors are directed perpendicular to or away from the solute. Thus, $\langle\Phi\rangle_0$ drops as

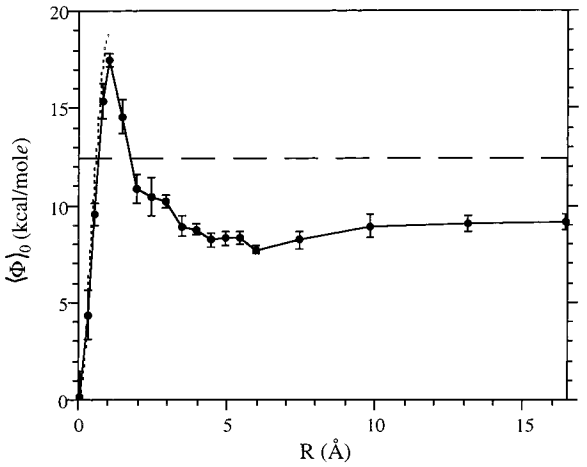

Figure 2. Electrostatic potential at the center of an uncharged solute cavity as a function of radius. The points are the simulation results with errors reported as 1 standard deviation. $\langle\Phi\rangle_0$ for the two largest cavities shown here (R = 13.15 and 16.45 Å) was evaluated from configuarations generated in a study mesoscopic hydrophobic cavities in water (Ashbaugh and Paulaitis, to be submitted for publication). The solid line is a guide for the eye. The short-dash line is the prediction of eq 5 for $R < R_{OH}$. The long-dash line is the vapor−water interfacial potential for SPC/E water ($\langle\Delta\Phi\rangle_{interface}$ = 12.3 kcal/mol calculated as the vapor potential minus the aqueous potential for comparison with the cavity potential).[25]

the hydrogens retreat from the solute to maintain the cage structure, reaching a minimum for solutes of intermediate size (4 Å < R < 7 Å). For even larger solutes (R > 7 Å), the hydration shell network is strained and water forfeits one hydrogen bond, thereby increasing the potential.[23] Indeed the potential increases weakly with increasing size for the largest solutes examined (Figure 2). Ultimately, the structure of water near a flat hydrophobic surface resembles a vapor−water interface,[24] at which point $\langle\Phi\rangle_0$ corresponds to the vapor−water interfacial potential.[25] Although beyond the scope of our analysis, this limit appears reasonable.

The Born equation provides an improved description of the charging free energies corrected for $\langle\Phi\rangle_0$ contributions, i.e., $\mu^*_{corrected} = \mu^*_{simulation} - q\langle\Phi\rangle_0 = -\int_0^q d\lambda' \int_0^{\lambda'}(\langle\Phi^2\rangle_\lambda - \langle\Phi\rangle_\lambda^2)\, d\lambda$. Below an ion radius of ∼8 Å the Born radii of cations and anions are linear with respect to R with slopes comparable to one (Figure 1). Cationic R_B evaluated from the corrected free energies are still greater than those of anions, largely since water hydrogens can penetrate the ion excluded volume and get closer to an anionic charge than oxygen is able to get to a cationic charge. Thus, interactions with anions, and subsequently the free energy, are more favorable. Interestingly, the corrected R_B of the largest monovalent cation and anion examined are indistinguishable from one another. The question follows: at what point do the cationic and anionic R_B become indistinguishable? Linearly extrapolating the simulation results for the smaller anions and cations, the R_B correlations converge at a physical ion radius of R^* = 8.5 ± 0.5 Å (Figure 1).[26] The simulations are not accurate enough, however, to asses whether the cation and anion correlations are distinct and simply cross each other, or follow a universal correlation applicable to both cations and anions for ions larger than R^*. By considering ions with fractional charge less than ±1e, R^* shifts to smaller values. For ions of charge ±0.5e the Born radii converge at R^* = 5.7 ± 0.3 Å (Figure 3). The Born radii of the larger cations and anions are indistinguishable, suggesting that above R^* the correlations

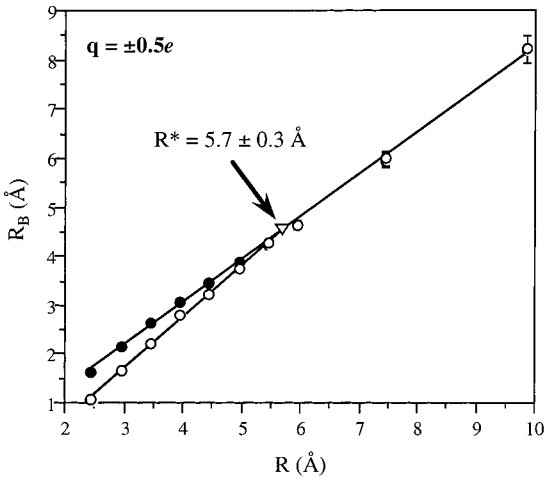

Figure 3. Born radii of half-valent ions corrected for $\langle\Phi\rangle_0$ contributions to the free energy. The symbols are defined in the caption to Figure 1.

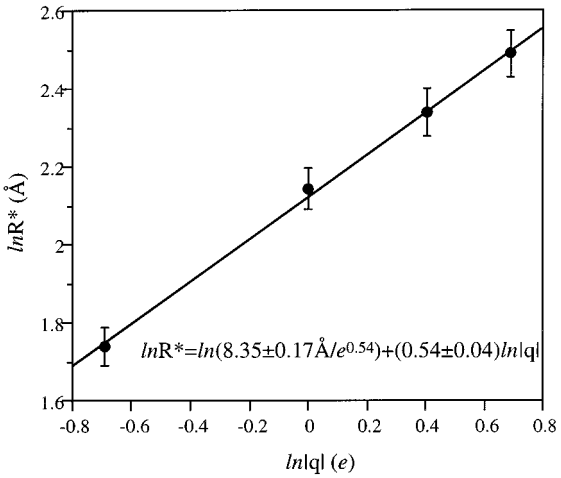

Figure 4. Dependence of the convergence radius R^* on the absolute ion charge. The points are the simulation results with errors reported as 1 standard deviation. The line is a power law fit of the simulation results.

merge into one. The fitted slope through the points greater than R^* is 0.92 ± 0.04, in reasonable agreement with the continuum prediction.

Subsequently, we ask how does R^* vary with ion charge? To this end, R^* has been determined for ions spanning charges from ±0.5e to ±2e.[26] Generally, R^* is an increasing function of charge (Figure 4). Assuming R^* is described by a power law, $R^* = \alpha|q|^\nu$, we obtain an exponent of υ = 0.54 ± 0.04 and prefactor of α = 8.35 ± 0.17 Å/$e^{0.54}$. To interpret this relationship, we compare R^* to the length scale characteristic of charge−water dipole interactions. Consider the energy required to flip a dipole from its average orientation about an ion at charge $+q$ to the average orientation it adopts about and ion of charge $-q$

$$U_{q\mu} = q\mu_w(\langle\cos\theta\rangle_{-q} - \langle\cos\theta\rangle_{+q})/r^2 \qquad (6)$$

where μ_w is the dipole moment of water (μ_{SPC} = 2.27 D), $\langle\cos\theta\rangle_q$ is the average projection of the dipole along the charge−ipole position vector with the ion at charge q, and r is the charge−dipole separation. Setting $U_{q\mu}$ equal to the thermal energy kT, the characteristic separation is

$$R_{q\mu}^{thermal} = |\mu_w\Delta\langle\cos\theta\rangle_{\mp q}/kT|^{0.5}|q|^{0.5} \qquad (7)$$

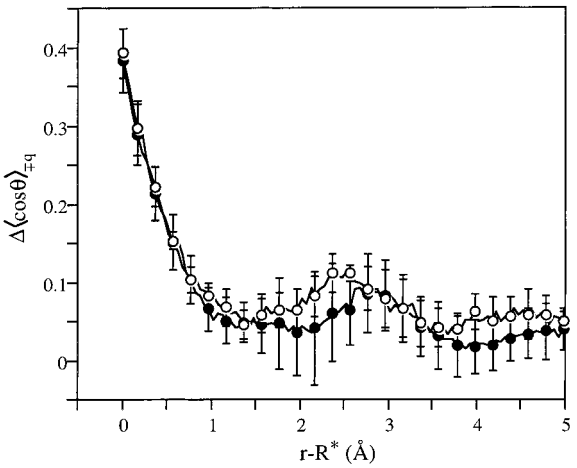

Figure 5. $\Delta\langle\cos\phi\rangle_{\mp q}$ ($= \langle\cos\theta\rangle_{-q} - \langle\cos\theta\rangle_{+q}$) as a function of distance for ions of radius R^* shifted to the left by R^*. The closed and open circles denote the results for the half- ($R^* = 5.7 \pm 0.3$ Å) and monovalent ($R^* = 8.5 \pm 0.5$ Å) ions, respectively. The error bars denote 1 standard deviation.

The derived power law exponent $\upsilon = 0.5$ agrees with the simulation result. In general, however, the polarization of water by an ion is a function of the ion charge and radius as well. Therefore $\Delta\langle\cos\theta\rangle_{\mp q}$ has been evaluated for the half- and monovalent ions of radius R^* (Figure 5). In the first hydration shell of the half- and monovalent ions the polarization of water is comparable. Most importantly, $\Delta\langle\cos\theta\rangle_{\mp q}$ at contact, i.e., at $r - R^* = 0$, is the same within the simulation error and equals 0.387 ± 0.036. Substituting this value of $\Delta\langle\cos\theta\rangle_{\mp q}$ into eq 7 yields 10.1 ± 0.5 Å/$e^{0.5}$ for the scaling prefactor for $R_{q\mu}^{\text{thermal}}$, only ~20% greater than that observed for R^*. The comparison between R^* and $R_{q\mu}^{\text{thermal}}$ assumes ion−dipole interactions in a vacuum are most significant, while multipolar and cooperative water−water interactions certainly play a role. Nonetheless, we believe the present analysis captures the essential underlying mechanism. For $R > R^*$, ion−water interactions in the first hydration shell are less than kT so that water configurations relevant to cation and anion hydration are sampled by thermal fluctuations. As a result, water does not discriminate between a cationic or anionic charge. For $R < R^*$, ion−water interactions are greater than kT and water adopts significantly different configurations about cations and anions due to the asymmetric structure of water. In this case, the predicted charge reversal symmetry breaks down and distinct R_B for cations and anions arise.

In conclusion, the continuum Born radii of atomic-sized anions and cations differ due to the stuctural asymmetry of water. When the ion is larger than the length scale for which ion−water dipole interactions compare to kT, Born radii for cations and anions converge and are indistinguishable. The present analysis has wider implications when applied to charged macromolecular species and surfaces, where R^* can be thought of as a critical surface charge density, $|q/4\pi R^{*2}| = 0.11$ e/nm^2, below which charge reversal symmetry and the continuum description of electrostatic potential fluctuations are accurate. Regardless of the solute size, however, the continuum model is unable to capture $\langle\Phi\rangle_0$ contributions to the free energy, which depend on the local solvation environment and can vary significantly near inhomogeneous structures such as proteins and solution phase boundaries.[25,27]

Acknowledgment. I thank Prof. Shekhar Garde and Dr. Gerhard Hummer for numerous insightful discussions.

References and Notes

(1) Honig, B.; Nicholls, A. *Science* **1995**, *268*, 1144.
(2) Born, M. *Z. Phys.* **1920**, *1*, 45.
(3) Hummer, G.; Pratt, L. R.; García, A. E. *J. Phys. Chem.* **1996**, *100*, 1206.
(4) Figuerido, F.; Del Buono, G. S.; Levy, R. M. *Biophys. Chem.* **1994**, *51*, 235.
(5) Åqvist, J.; Hansson, T. *J. Phys. Chem.* **1996**, *100*, 9512.
(6) Garde, S.; Hummer, G.; Paulaitis, M. E. *J. Chem. Phys.* **1998**, *108*, 1552.
(7) Hummer, G.; Pratt, L. R.; García, A. E. *J. Am. Chem. Soc.* **1997**, *119*, 8523.
(8) Hummer, G.; Pratt, L. R.; García, A. E. *J. Phys. Chem. A* **1998**, *102*, 7885.
(9) Rick, S.; Berne, B. J. *J. Am. Chem. Soc.* **1994**, *116*, 3949.
(10) Hummer, G.; Pratt, L. R.; García, A. E. *J. Phys. Chem.* **1995**, *99*, 14188.
(11) Latimer, W. M.; Pitzer, K. S.; Slansky, C. M. *J. Chem. Phys.* **1939**, *7*, 108.
(12) Rashin, A. A.; Honig, B. *J. Phys. Chem.* **1985**, *89*, 5588.
(13) Sitkoff, D.; Ben-Taul, N.; Honig, B. *J. Phys. Chem.* **1996**, *100*, 2744.
(14) Babu, C. S.; Lim, C. *Chem. Phys. Lett.* **1999**, *310*, 225.
(15) Schmid, R.; Miah, A. M.; Sapunov, V. N. *Phys. Chem. Chem. Phys.* **2000**, *2*, 97.
(16) Berendsen, H. J. C.; Postma, J. P. M.; van Gunsteren, W. F.; Hermans, J. In *Intermolecular Forces: Proceedings of the Fourteenth Jerusalem Symposium on Quantum Chemistry and Biochemistry*; Pullman, B., Ed.; D. Reidel Publishing Co.: Dordrecht, Holland, 1981; Vol. p 331.
(17) Hummer, G.; Szabo, A. *J. Chem. Phys.* **1996**, *105*, 2004.
(18) DeLeeuw, S. W.; Perram, J. W.; Smith, E. R. *Proc. R. Soc. London* **1980**, *A373*, 27.
(19) Hummer, G.; Pratt, L. R.; García, A. E.; Garde, S.; Berne, B. J.; Rick, S. W. *J. Phys. Chem. B* **1998**, *102*, 3841.
(20) Hummer, G.; Pratt, L. R.; García, A. E. *J. Chem. Phys.* **1997**, *107*, 9275.
(21) Sakane, S.; Ashbaugh, H. S.; Wood, R. H. *J. Phys. Chem. B* **1998**, *102*, 5673.
(22) From the Born equation, $\langle\Phi^2\rangle - \langle\Phi\rangle^2 = kT(1 - 1/\epsilon)/R_B$. While not quantitative, the conclusions that $\langle\Phi^2\rangle - \langle\Phi\rangle^2$ is independent of q and monotonically decreases with size are qualitatively correct.
(23) Lee, C. Y.; McCammon, J. A.; Rossky, P. J. *J. Chem. Phys.* **1984**, *80*, 4448.
(24) Stillinger, F. H. *J. Solution Chem.* **1973**, *2*, 141.
(25) Sokhan, V. P.; Tildesley, D. J. *Mol. Phys.* **1997**, *92*, 625.
(26) R^* was determined by linearly extrapolating R_B for anions and cations. Linear cation and anion correlations were obtained by fitting to the six consecutive points immediately below R^*. In the case of $q = \pm 2e$ the fitted lines had to be extrapolated a little over 2 Å to obtain R^*.
(27) Ashbaugh, H. S. *Mol. Phys.* **1999**, *97*, 433.